

An intranasal lentiviral booster reinforces the waning mRNA vaccine-induced SARS-CoV-2 immunity that it targets to lung mucosa

Benjamin Vesin,^{1,7} Jodie Lopez,^{1,7} Amandine Noirat,^{1,7} Pierre Authié,^{1,7} Ingrid Fert,¹ Fabien Le Chevalier,¹ Fanny Moncoq,¹ Kirill Nemirov,¹ Catherine Blanc,¹ Cyril Planchais,² Hugo Mouquet,² Françoise Guinet,³ David Hardy,⁴ Francina Langa Vives,⁵ Christiane Gerke,⁶ François Anna,¹ Maryline Bourguine,¹ Laleh Majlessi,^{1,8} and Pierre Charneau^{1,8}

¹Pasteur-TheraVectys Joint Lab, Institut Pasteur, Virology Department, 28 rue du Dr. Roux, Paris F-75015, France; ²Laboratory of Humoral Immunology, Université de Paris, Immunology Department, Institut Pasteur, INSERM U1222, Paris F-75015, France; ³Lymphocytes and Immunity Unit, Université de Paris, Immunology Department, Institut Pasteur, Paris F-75015, France; ⁴Histopathology Platform, Institut Pasteur, Paris F-75015, France; ⁵Mouse Genetics Engineering, Institut Pasteur, Paris F-75015, France; ⁶Institut Pasteur, Université de Paris, Innovation Office, Vaccine Programs, Institut Pasteur, Paris F-75015, France

As the coronavirus disease 2019 (COVID-19) pandemic continues and new severe acute respiratory syndrome coronavirus 2 (SARS-CoV-2) variants of concern emerge, the adaptive immunity initially induced by the first-generation COVID-19 vaccines starts waning and needs to be strengthened and broadened in specificity. Vaccination by the nasal route induces mucosal, humoral, and cellular immunity at the entry point of SARS-CoV-2 into the host organism and has been shown to be the most effective for reducing viral transmission. The lentiviral vaccination vector (LV) is particularly suitable for this route of immunization owing to its non-cytopathic, non-replicative, and scarcely inflammatory properties. Here, to set up an optimized cross-protective intranasal booster against COVID-19, we generated an LV encoding stabilized spike of SARS-CoV-2 Beta variant (LV::S_{Beta-2P}). mRNA vaccine-primed and -boosted mice, with waning primary humoral immunity at 4 months after vaccination, were boosted intranasally with LV::S_{Beta-2P}. A strong boost effect was detected on cross-sero-neutralizing activity and systemic T cell immunity. In addition, mucosal anti-spike IgG and IgA, lung-resident B cells, and effector memory and resident T cells were efficiently induced, correlating with complete pulmonary protection against the SARS-CoV-2 Delta variant, demonstrating the suitability of the LV::S_{Beta-2P} vaccine candidate as an intranasal booster against COVID-19. LV::S_{Beta-2P} vaccination was also fully protective against Omicron infection of the lungs and central nervous system, in the highly susceptible B6.K18-hACE2^{IP-THV} transgenic mice.

INTRODUCTION

Considering (i) the sustained pandemicity of coronavirus disease 2019 (COVID-19), (ii) weakening protection potential of the first-generation vaccines against severe acute respiratory syndrome beta-coronavirus 2 (SARS-CoV-2), and (iii) the ceaseless emergence of

new viral variants of concern (VOCs), new effective vaccine platforms can be critical for future primary or booster vaccines.¹ We recently demonstrated the strong performance of a non-integrative lentiviral vaccination vector (LV) encoding the full-length sequence of the spike glycoprotein (S) from the ancestral SARS-CoV-2 (LV::S), when used in systemic prime followed by an intranasal (i.n.) boost in multiple preclinical models.² LV::S ensures complete (cross-) protection of the respiratory tract against ancestral SARS-CoV-2 and VOCs.³ In addition, in our new transgenic mice expressing human angiotensin-converting enzyme 2 (hACE2) and displaying unprecedented permissiveness of the brain to SARS-CoV-2 replication, an i.n. boost with LV::S is required for full protection of the central nervous system.³ LV::S is intended to be used as a booster for individuals who already have been vaccinated against and/or infected by SARS-CoV-2, to reinforce and broaden protection against emerging VOCs with immune evasion potential.⁴

Vaccine LVs are non-integrating, non-replicative, non-cytopathic, and negligibly inflammatory.^{5,6} These vectors are pseudotyped with the heterologous glycoprotein from the vesicular stomatitis virus (VSV-G), which confers them a broad tropism for various cell types, including dendritic cells. The latter are mainly non-dividing cells and thus usually hardly permissive to gene transfer. However, LVs possess the crucial ability to efficiently transfer genes to the nuclei of not only dividing, but also of non-dividing cells, therefore making efficient transduction of non-dividing immature dendritic cells possible. The resulting endogenous antigen expression in dendritic cells, with their

Received 13 February 2022; accepted 22 April 2022;
<https://doi.org/10.1016/j.ymthe.2022.04.016>

⁷These authors contributed equally

⁸Senior authors

Correspondence: Laleh Majlessi, Ph.D. Pasteur-TheraVectys Joint Lab, Institut Pasteur, Virology Department, 28 rue du Dr. Roux, Paris 75015, France.

E-mail: laleh.majlessi@pasteur.fr

unique ability to activate naive T cells,⁷ correlates with a strong induction of high-quality effector and memory T cells.⁸ Importantly, the VSV-G pseudo-typing of LVs prevents them from being targets of pre-existing vector-specific immunity in humans, which is key in vaccine development.^{5,6} The safety of LVs has been established in humans in a phase I/IIa HIV-1 therapeutic vaccine trial, although the LV used in that clinical trial had been an integrative version.⁹ Because of their non-cytopathic and non-inflammatory properties,¹⁰ (J.L. and L.M., unpublished observation), LVs are well suited for mucosal vaccination. The i.n. immunization approach is expected to trigger mucosal IgA responses, as well as resident B and T lymphocytes in the respiratory tract.¹¹ This immunization route has also been shown to be the most effective at reducing SARS-CoV-2 transmission in both hamster and macaque preclinical models.¹² The induction of mucosal immunity by i.n. immunization allows SARS-CoV-2 neutralization directly at the gateway to the host organism, before it gains access to major infectable anatomical sites.²

The duration of the protection conferred by the first generation COVID-19 vaccines is not yet well established, hardly predictable with serological laboratory tests, and inconsistent among individuals and against distinct VOCs. Despite high vaccination rates, the current exacerbation of the world-wide pandemic indicates that repeated booster immunizations will be needed to ensure individual and collective immunity against COVID-19. In this context, the safety and potential adverse effects of multiple additional homologous doses of the first-generation COVID-19 vaccines, for instance related to allergic reaction to polyethylene glycol contained in mRNA vaccines, have to be considered.¹³ Importantly, a heterologous prime boost vaccine delivery method has been proven to be a more successful strategy than the homologous prime boost approach in numerous preclinical models of various infectious diseases.^{14–16} Therefore, new efficient vaccination platforms are of particular interest to develop heterologous boosters against COVID-19. The LV::S vaccine candidate has the potential for prophylactic use against COVID-19, mainly based on its powerful capacity to induce not only strong neutralizing humoral responses, but also, and most important, robust protective T cell responses, which preserve their immune detection of spike from SARS-CoV-2 VOCs, despite the accumulation of escape mutations.³ The basis for the immunogenicity of LVs is usually the genetic message they deliver to host cells and that encodes the targeted antigen. However, in the particular case of viral envelope proteins used as antigens, which comprise the transmembrane and the tail segments, it cannot be excluded that the LV is pseudotyped by both VSV-G and the viral envelope protein they encode. In the context of LV::SFL, the possible spike glycoprotein on the LV surface may contribute to the induction of immune responses, in addition to the genetic message that is translated and expressed by the antigen presenting cells. LV::S is remarkably suited to be used as a heterologous i.n. booster vaccine, to reinforce and broaden protection against the emerging VOCs, while collective immunity in early vaccinated nations is waning a few months after completion of the initial immunizations and while new waves of infections are on the rise.⁴

In the present study, toward the preparation of a clinical trial, we first generated an LV encoding the down-selected S_{CoV-2} of the Beta variant, stabilized by K^{986P} and V^{987P} substitutions in the S2 domain of S_{CoV-2} (LV::S_{Beta-2P}). In mice, primed and boosted intramuscularly (i.m.) with mRNA vaccine encoding for the ancestral S_{CoV-2}^{17,18} and in which the (cross-) sero-neutralization potential was progressively decreasing, we investigated the systemic and mucosal immune responses and the protective potential of an i.n. LV::S_{Beta-2P} heterologous boost.

RESULTS

Antigen design and down-selection of a lead candidate

To select the most suitable S_{CoV-2} variant to induce the greatest neutralization breadth based on the known variants, we generated LVs encoding the full-length S_{CoV-2} from the Alpha, Beta, or Gamma SARS-CoV-2 VOCs. C57BL/6 mice (n = 5/group) were primed i.m. (week 0) and boosted i.m. (week 3) with 1×10^8 TU/mouse of each individual LV and the (cross-) neutralization potential of their sera was assessed before boost (week 3) and after boost (week 5) against pseudoviruses carrying various S_{CoV-2} (Figure 1A). These pseudo-viruses are LV particles that carry the spike of interest on their surface, but do not have the genetic message for the spike and should not be confused with the LV-based vaccine that carries the genetic message-encoding spike. Immunization with LV::S_{Alpha} generated appropriate neutralization capacity against S_{D614G} and S_{Alpha} but not against S_{Beta} and S_{Gamma} (Figure 1B). Between LV::S_{Beta} and LV::S_{Gamma}, the former generated the highest cross-sero-neutralization potential against the S_{D614G}, S_{Alpha}, and S_{Gamma} variants. In accordance with previous observations using other vaccination strategies, in the context of immunization with LV, the K^{986P} - V^{987P} substitutions in the S2 domain of S_{CoV-2} improved the (cross-) sero-neutralization potential (Figure 1C), probably owing to an extended half-life of S_{CoV-2-2P}.¹⁹

Taken together, these data allowed to down-select S_{Beta-2P} as the best cross-reactive antigen candidate to be used in the context of LV (LV::S_{Beta-2P}) to strengthen the waning immunity previously induced by the first-generation COVID-19 vaccines, like mRNA. Although, the comparison between the WT and 2P forms was performed here with the D614G sequence, stabilization by the 2P substitution is so well documented¹⁹ that an extrapolation to S_{Beta} seemed well founded.

Follow-up of humoral immunity in mRNA-primed and -boosted mice and the effect of an LV::S_{Beta-2P} i.n. boost

We analyzed the potential of LV::S_{Beta-2P} i.n. boost vaccination to strengthen and broaden the immune responses in mice that were initially primed and boosted with mRNA and in which the (cross-) sero-neutralization potential was decreasing. C57BL/6 mice were primed i.m. at week 0 and boosted i.m. at week 3 with 1 µg/mouse of mRNA (Figure 2A). In mRNA-primed mice, serum anti-S_{CoV-2} and anti-RBD IgG were detected at week 3, increased after mRNA boost as studied at weeks 6 and 10, and then decreased at week 17 in the absence of an additional boost (Figure S1A).

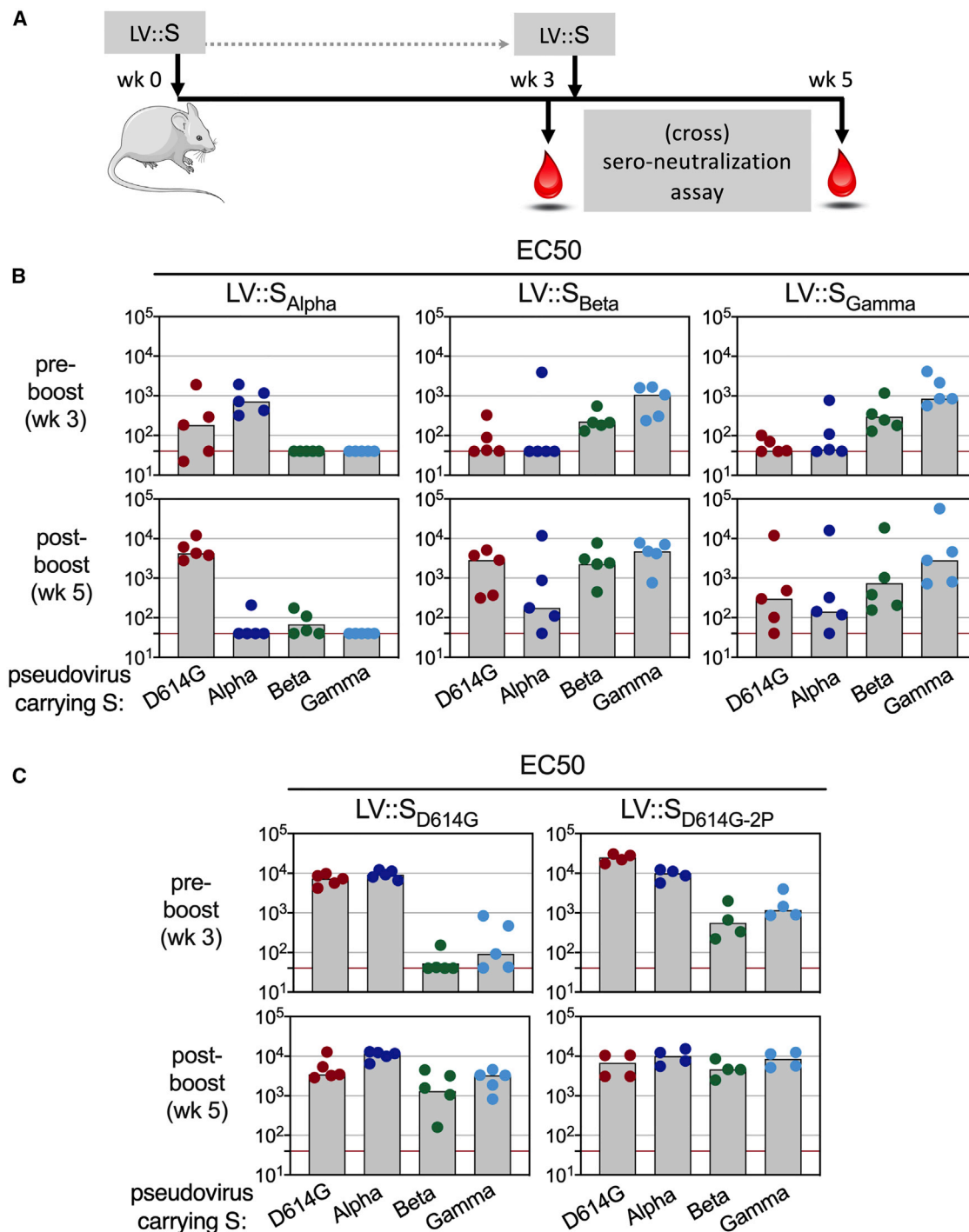
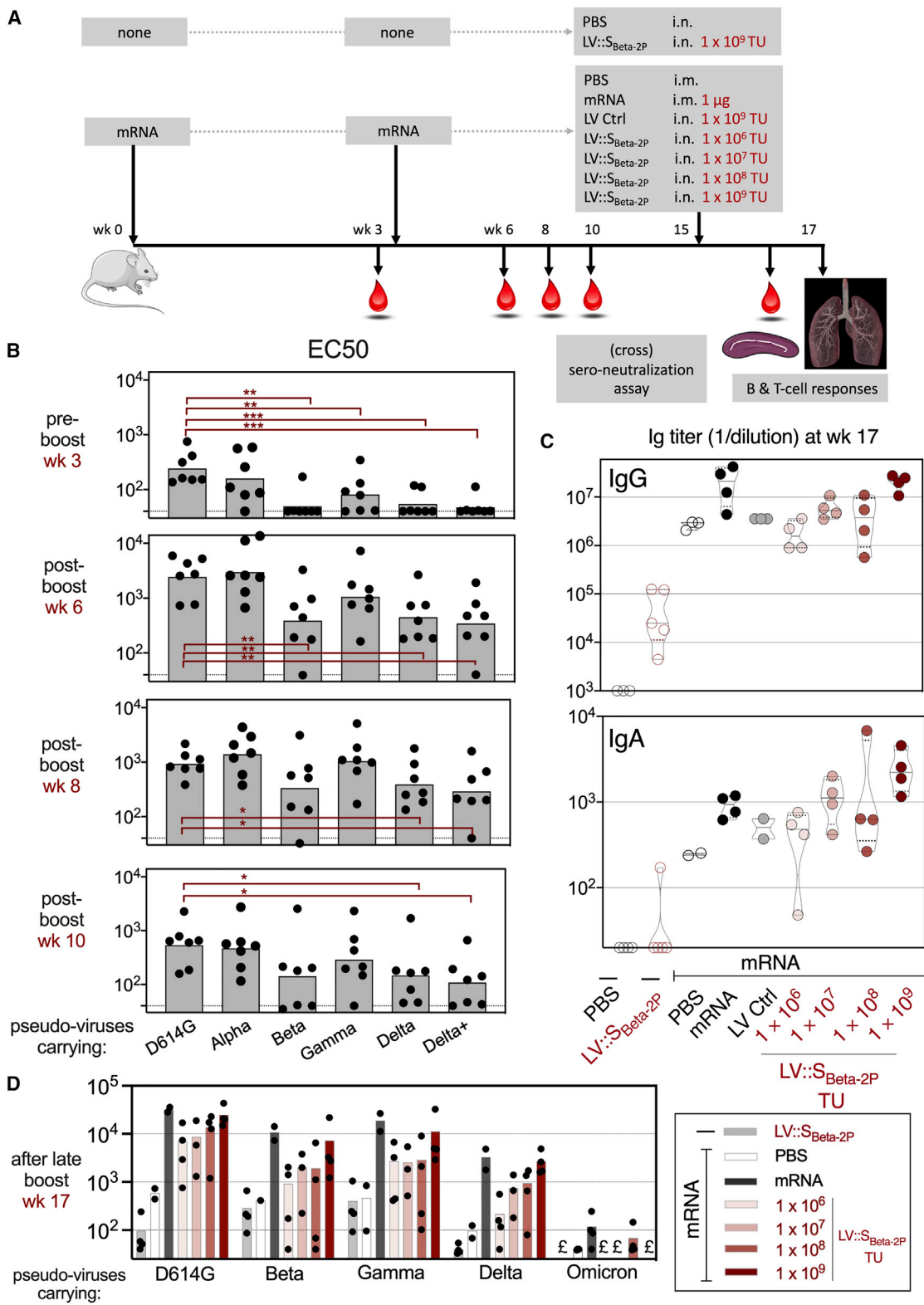


Figure 1. Down-selection of a S_{Cov-2} variant with the highest potential to induce cross-sero-neutralizing antibodies

(A) Timeline of prime-boost vaccination with LV::S_{Alpha}, LV::S_{Beta} or LV::S_{Gamma} and (cross-) sero-neutralization assays in C57BL/6 mice (n = 4–5/group). (B) The median effective concentration (EC₅₀) of neutralizing activity of sera from vaccinated mice was evaluated before and after the boost, against pseudo-viruses carrying S_{Cov-2} from D614G, Alpha, Beta, or Gamma variants. (C) The EC₅₀ of sera from C57BL/6 mice, vaccinated following the regimen detailed in (A) with LV encoding for S_{D614G}, either WT or carrying the K⁹⁸⁶P - V⁹⁸⁷P substitutions in the S2 domain. The EC₅₀ was evaluated before and after the boost, as indicated in (B).



(legend on next page)

Longitudinal serological follow-up demonstrated that at 3 weeks after prime, cross-neutralization activities against both S_{D614G} and S_{Alpha} were readily detectable (Figure 2B). Cross-sero-neutralization was also detectable, although to a lesser degree, against S_{Gamma}, but not against S_{Beta}, S_{Delta}, or S_{Delta+}. At week 6, i.e., 3 weeks post boost, cross-sero-neutralization activities against all S_{CoV-2} variants were detectable, although at significantly lesser extents against S_{Beta}, S_{Delta}, and S_{Delta+}. From week 6 to week 10, cross-sero-neutralization against S_{Beta}, S_{Delta}, or S_{Delta+} gradually and significantly decreased. At week 10, one-half of the mice lost the cross-sero-neutralization potential against S_{Beta}, S_{Delta}, or S_{Delta+} (Figure 2B).

At week 15, groups of mRNA-primed and -boosted mice were injected i.m. with 1 µg of mRNA vaccine or PBS. The dose of 1 µg of mRNA per mouse has been demonstrated to be fully protective in mice.²⁰ In parallel, at this time point, mRNA-primed and -boosted mice received i.n. 1×10^9 transduction units (TU)/mouse of an empty LV (LV Ctrl) or escalating doses of 1×10^6 , 1×10^7 , 1×10^8 , or 1×10^9 TU of LV::S_{Beta-2P} (Figure 2A). Unprimed, age-matched mice received i.n. 1×10^9 TU of LV::S_{Beta-2P} or PBS.

In the previously mRNA-primed and -boosted mice, injected at week 15 with a third dose of mRNA or with 1×10^8 or 1×10^9 TU of LV::S_{Beta-2P}, marked anti-S_{CoV-2} IgG titer increases were observed (Figure 2C). The titers of anti-S_{CoV-2} IgA were higher in the mice injected with 1×10^9 TU of LV::S_{Beta-2P} than those injected with a third 1-µg dose of an mRNA vaccine (Figure 2C). In agreement with these results, (cross-) sero-neutralization activity increased in a dose-dependent manner with LV::S_{Beta-2P} i.n. boost given at week 15, as studied at week 17 (Figure 2D). Of note, cross-sero-neutralization activity against S_{Omicron}-carrying pseudo-viruses was very low in mRNA-primed and -boosted mice injected at week 15 with a third dose of mRNA via i.m. or with 1×10^8 TU of LV::S_{Beta-2P} i.n. At the mucosal level, at this time point, titers of anti-S_{CoV-2} and anti-RBD IgG in the total lung extracts increased in a dose-dependent manner in LV::S_{Beta-2P}-boosted mice, and the titer obtained with the highest dose of LV::S_{Beta-2P} was comparable with that after the third 1-µg i.m. dose of an mRNA vaccine (Figure S1B). Importantly, significant titers of lung anti-S_{CoV-2} IgA were only detected in LV::S_{Beta-2P}-boosted mice (Figure S1B).

At the lung cellular level, CD19⁺ B cells, which are class switched and thus surface IgM⁻/IgD⁻ plasma cells, and that express CD38, CD62L, CD73, and CD80, can be defined as lung resident B cells (Brm)^{21,22} (Figure 3A). The proportion of these B cells increased in a dose-dependent manner in the lungs of mice boosted i.n. with LV::S_{Beta-2P} (Figure 3B). Mucosal anti-S_{CoV-2} IgA and Brm were barely detectable in the mice boosted i.m. at week 15 with 1 µg

mRNA, which was the single dose of RNA tested in our experiment and thus serves only as indication.

Systemic and mucosal T cell immunity after i.n. LV::S_{Beta-2P} boost in previously mRNA-primed and -boosted mice

Mice were primed and boosted with 1 µg mRNA vaccine and then boosted i.n. at week 15 with escalating doses of LV::S_{Beta-2P}, according to the above-mentioned regimen (Figure 2A). At week 17, i.e., 2 weeks after the late boost, systemic anti-S_{CoV-2} T cell immunity was assessed by interferon (IFN)-γ-specific ELISPOT in the spleen of individual mice after *in vitro* stimulation with individual S:256-275, S:536-550, or S:576-590 peptide, encompassing immunodominant S_{CoV-2} regions for CD8⁺ T cells in H-2^b mice.² Importantly, the weak anti-S CD8⁺ T cell immunity, detectable in the spleens of mRNA-primed and -boosted mice at week 17, largely increased after the i.n. boost with 1×10^8 and 1×10^9 TU of LV::S_{Beta-2P}, similar to the increase after i.m. mRNA boost (Figure 4).

In parallel, in the same animals, the mucosal anti-S_{CoV-2} T cell immunity was assessed by intracellular Tc1 and Tc2 cytokine staining in T cell-enriched fractions from individual mice after *in vitro* stimulation with autologous bone marrow dendritic cells loaded with a pool of S:256-275, S:536-550, and S:576-590 peptides (Figure 5). In previously mRNA-primed and -boosted mice, only a few S_{CoV-2}-specific IFN-γ/tumor necrosis factor (TNF)/IL-2 CD8⁺ T cell responses were detected in the lungs (Figure 5). However, the i.n. administration of LV::S_{Beta-2P} boosted, these Tc1 responses in a dose-dependent manner. Sizable percentages of these Tc1 cells were induced with 1×10^8 or 1×10^9 TU LV::S_{Beta-2P}. mRNA (1 µg) i.m. administration had a substantially lower boost effect on mucosal T cells (Figure 5). Tc2 responses (IL-4, IL-5, IL-10, and IL-13) were not detected in any experimental group (Figure S2), as assessed in the same lung T cell cultures.

Mucosal lung resident memory T cells (Trm), CD8⁺ CD44⁺ CD69⁺ CD103⁺ which are one of the best correlates of protection in infectious diseases,²³ were readily detected in the mice boosted i.n. with 1×10^8 or 1×10^9 TU of LV::S_{Beta-2P} (Figures 6A and 6B). No Trm were detected in the lungs of mice boosted late with 1 µg mRNA i.m..

Features of lungs after LV::S_{Beta-2P} i.n. administration

To identify the immune cell subsets transduced *in vivo* by LV after i.n. administration, C57BL/6 mice were immunized i.n. with the high dose of 1×10^9 TU of LV::GFP or LV::nano-Luciferase as a negative control. Lungs were collected at 4 days after immunization and analyzed by cytometry in individual mice. CD45⁻ cell subset was devoid of GFP⁺ cells. Only very few GFP⁺ cells were detected in the

Figure 2. Anti-S_{CoV-2} humoral responses in mRNA-vaccinated mice, which were further i.n. boosted with LV::S_{Beta-2P}

(A) Timeline of mRNA i.m.-i.m. prime-boost vaccination in C57BL/6 mice which were later immunized i.n. by escalating doses of LV::S_{Beta-2P} ($n = 4-5$ /group) and the (cross) sero-neutralization follow-up. (B) Serum median effective concentration (EC₅₀) determined at the indicated time points against pseudo-viruses carrying S_{CoV-2} from D614G, Alpha, Beta, Gamma, Delta, or Delta+ variants. (C) Anti-S_{CoV-2} IgG (top) or IgA (bottom) titers in the sera 2 weeks after i.n. LV::S_{Beta-2P} boost. Statistical significance was determined by Mann-Whitney test (* $p < 0.05$, ** $p < 0.01$, *** $p < 0.001$). (D) Sera EC₅₀, after the late boost given at week 15, and as determined at week 17. $\text{E} =$ not determined.

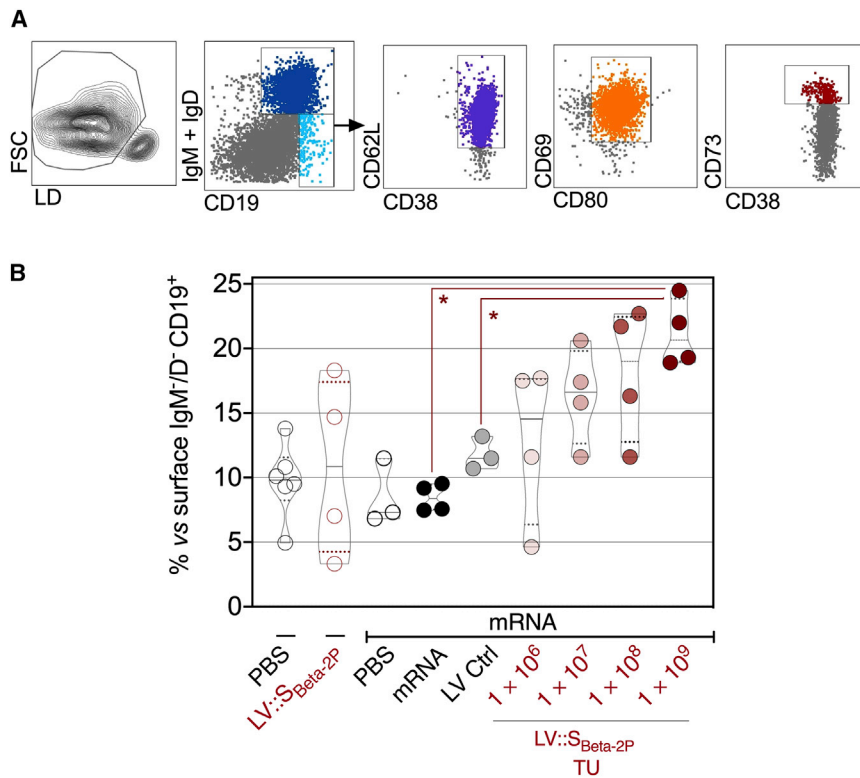


Figure 3. Lung B cell resident memory subset in mRNA-vaccinated mice that were further i.n. boosted with LV::S_{Beta-2P}

The mice are those detailed in Figure 2. Mucosal immune cells were studied 2 weeks after LV::S_{Beta-2P} i.n. boost. (A) Cytometric gating strategy to detect lung Bm in mRNA-vaccinated mice which were further i.n. boosted with LV::S_{Beta-2P}. (B) Percentages of these cells among lung CD19⁺ surface IgM⁻/IgD⁻ B cells in mRNA-vaccinated mice that were further i.n. boosted with LV::S_{Beta-2P}. Statistical significance was determined by Mann-Whitney test (*p < 0.05).

CD45⁺ hematopoietic cells (Figures S3A–S3C). The CD45⁺ GFP⁺ cells were located in a CD11b^{hi} subset and in the CD11b^{int} CD11c⁺ CD103⁺ MHC-II⁺ (dendritic cells) (Figure S3B).

To evaluate possible lung infiltration after LV i.n. administration, C57BL/6 mice were injected i.n. with the high dose of 1×10^9 TU of LV::S_{Beta-2P} or PBS as a negative control. Lungs were collected at 1, 3 or 14 days after injection for histopathological analysis. Hematoxylin and eosin (H&E) histological sections displayed minimal to moderate inflammation, interstitial and alveolar syndromes in both experimental groups, regardless of the three time points investigated. No specific immune infiltration or syndrome was detected in the animals treated i.n. with 1×10^9 TU of LV::S_{Beta-2P}, compared with PBS (Figures S4A and S4B).

Protection of lungs in mRNA-primed and -boosted mice, and later boosted i.n. with LV::S_{Beta-2P}

We then evaluated the protective vaccine efficacy of LV::S_{Beta-2P} i.n. in mRNA-primed and -boosted mice. At week 15, mRNA-primed and -boosted mice received i.m. 1 μg mRNA or PBS. In parallel, mRNA-primed and -boosted mice received i.n. 1×10^8 TU LV::S_{Beta-2P} or control empty LV (Figure 7A). The choice of this dose was based on our previous experience in which this dose was fully effective in protection in homologous LV::S prime-boost regimens,^{2,3} even though it does not result in the strongest immune responses. Unvaccinated, age- and sex-matched controls were left unimmunized. Five weeks after the late boost, i.e., at week 20, all mice

were pre-treated with 3×10^8 infectious genome units (IGU) of an adenoviral vector serotype 5 encoding hACE2 (Ad5::hACE2)² to render their lungs permissive to SARS-CoV-2 replication (Figure 7A). Four days later, mice were challenged with the SARS-CoV-2 Delta variant, which at the time of this study, i.e., November 2021, was the dominant SARS-CoV-2 variant worldwide.

At day 3 after infection, a primary analysis of the total lung RNA showed that hACE2 mRNA was similarly expressed in all mice after Ad5::hACE2 *in vivo* transduction (Figure 7B).

Lung viral loads were then determined at 3 days after infection by assessing total E RNA and sub-genomic (Esg) E_{CoV-2} RNA quantitative reverse transcriptase PCR (qRT-PCR), the latter being an indicator of active viral replication.^{24–26} In mice initially primed and boosted with mRNA vaccine and then injected i.n. with the control LV or i.m. with PBS, no significant protective capacity was detectable (Figure 7C). In contrast, the LV::S_{Beta-2P} i.n. boost of the initially mRNA vaccinated mice drastically decreased the total E RNA content of SARS-CoV-2 and no copies of the replication-related Esg E_{CoV-2} RNA were detected in this group (Figure 7C). In the group that received a late mRNA i.m. boost, the total E RNA content was also significantly reduced and the content of the Esg E_{CoV-2} RNA was undetectable in three of five mice in this group.

Therefore, a late LV::S_{Beta-2P} heterologous i.n. boost, given at week 15 after the first injection of mRNA, at the dose of 1×10^8 TU/mouse resulted in complete protection, i.e., total absence of viral replication in 100% of animals, against a high-dose challenge with the SARS-CoV-2 Delta variant.

Full cross-protective capacity of LV::S_{Beta-2P} against SARS-CoV-2 Omicron BA.1 variant

Given the timing of the lengthy preparation of mRNA-primed and -boosted mice, again boosted i.n. with LV::S_{Beta-2P} at week 15 (July to November 2021), and the emergence of the Omicron variant (December 2021), it was not possible for us to evaluate the anti-Omicron cross-protection potential of LV::S_{Beta-2P} used as a late i.n.

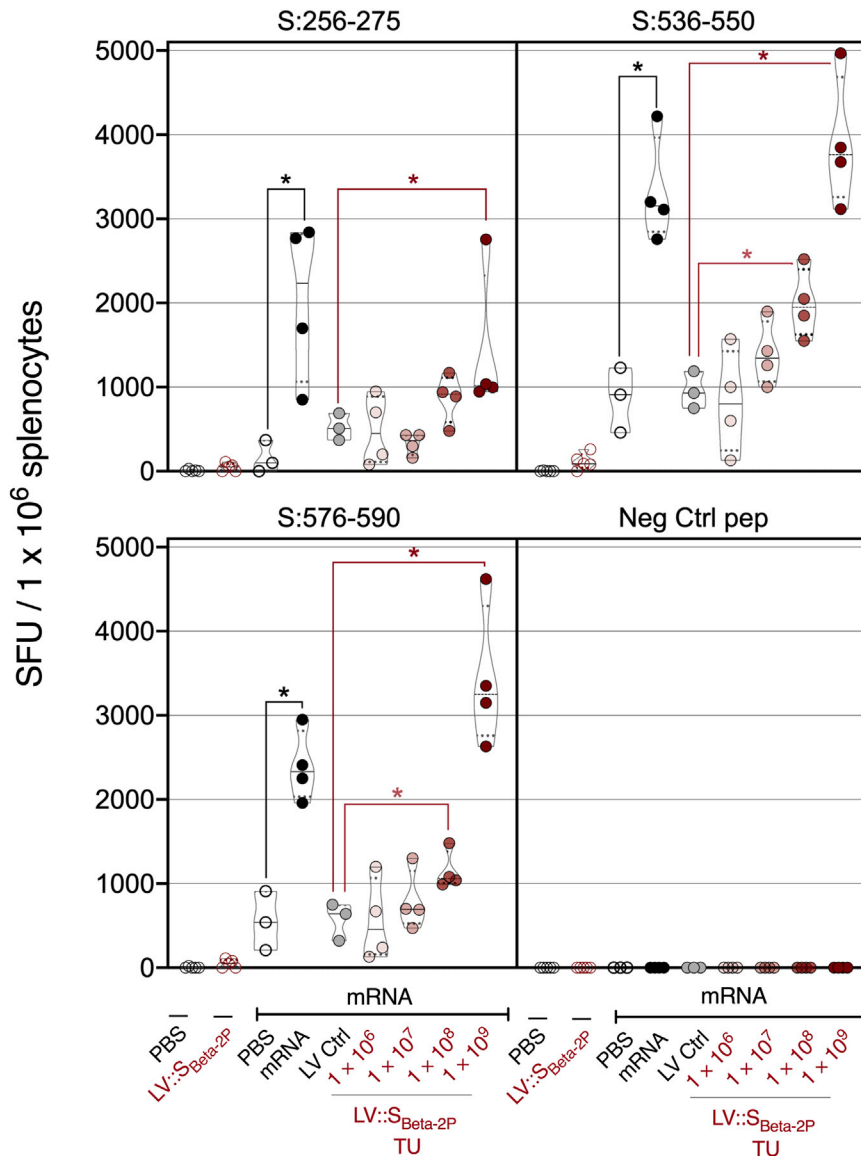


Figure 4. Systemic CD8⁺ T cell responses to SCoV-2 in mRNA-vaccinated mice that were further i.n. boosted with LV::SBeta-2P

The mice are those detailed in Figure 2. T-splenocyte responses were evaluated 2 weeks after LV::SBeta-2P i.n. boost by IFN- γ ELISPOT after stimulation with S:256-275, S:536-550, or S:576-590 synthetic 15-mer peptides encompassing SCoV-2 MHC-I-restricted epitopes. Statistical significance was evaluated by the Mann-Whitney test (* $p < 0.05$).

the six others showed significant replication in the brain. Therefore, the LV::SBeta-2P displays a full cross-protective capacity against the Omicron variant, which is fully comparable with its efficiency against the ancestral^{2,3} or the Delta variant.

DISCUSSION

With the weakly persistent prophylactic potential of the immunity initially induced by the first-generation COVID-19 vaccines, especially against new VOCs, the administration of additional vaccine doses becomes essential.¹ As an alternative to additional doses of the same vaccines, combining vaccine platforms in a heterologous prime-boost regimen holds promise for gaining protective efficacy.²⁸ Compared with homologous vaccine dose administrations, heterologous prime-boost strategies may reinforce more efficiently specific adaptive immune responses and long-term protection.²⁹ Furthermore, the sequence of the spike antigen has to be adapted according to the dynamics of SARS-CoV-2 VOC emergence to induce the greatest neutralization breadth. Protection against symptomatic SARS-CoV-2 infection is mainly related to sero-neutralizing activity,

while CD8⁺ T cell immunity, with their ability to cytolize virus-infected cells, especially control the virus replication and result in the resolution of viral infection.³⁰ Therefore, an appropriate B and T cell vaccine platform, including an adapted SCoV2 sequence, is of utmost interest at the current step of the pandemic.

The LV-based strategy is highly efficient, not only in inducing humoral responses, but also, and particularly, in establishing high-quality and memory T cell responses.⁸ This makes it a suitable platform for a heterologous boost, even if it is also largely efficacious on its own as a primary COVID-19 vaccine candidate.^{2,3} Furthermore, LVs are non-cytopathic, non-replicative, and scarcely inflammatory. They can thus be used to perform a non-invasive i.n. boost to efficiently induce sterilizing mucosal immunity, which protects the respiratory system as well as the central nervous system.^{2,3} The i.n. route of

boost in parallel. However, we evaluated the protective efficacy of LV::SBeta-2P in the very sensitive B6.K18-hACE2^{IP-THV} transgenic mice, which are prone to SARS-CoV-2 infection in the lung, and in addition display unprecedented brain permissiveness to SARS-CoV-2 replication.³ B6.K18-hACE2^{IP-THV} mice ($n = 5-8$ /group) were primed i.m. with 1×10^8 TU/mouse of LV::SBeta-2P or an empty LV at week 0 and then boosted i.n. at week 3 with the same dose of the same vectors (Figure 8A). Mice were then challenged (i.n.) with 0.3×10^5 TCID₅₀ of a SARS-CoV-2 Omicron BA.1 variant²⁷ at week 5. Lung and brain viral RNA contents were then determined at day 5 after infection by using Esg ECoV-2 RNA qRT-PCR. LV::SBeta-2P vaccination-conferred sterilizing protection against SARS-CoV-2 Omicron in the lungs and brain *versus* high rates of viral replication in the sham-vaccinated controls (Figure 8B). Of note, even if two mice out of eight did not show cervical infection with Omicron,

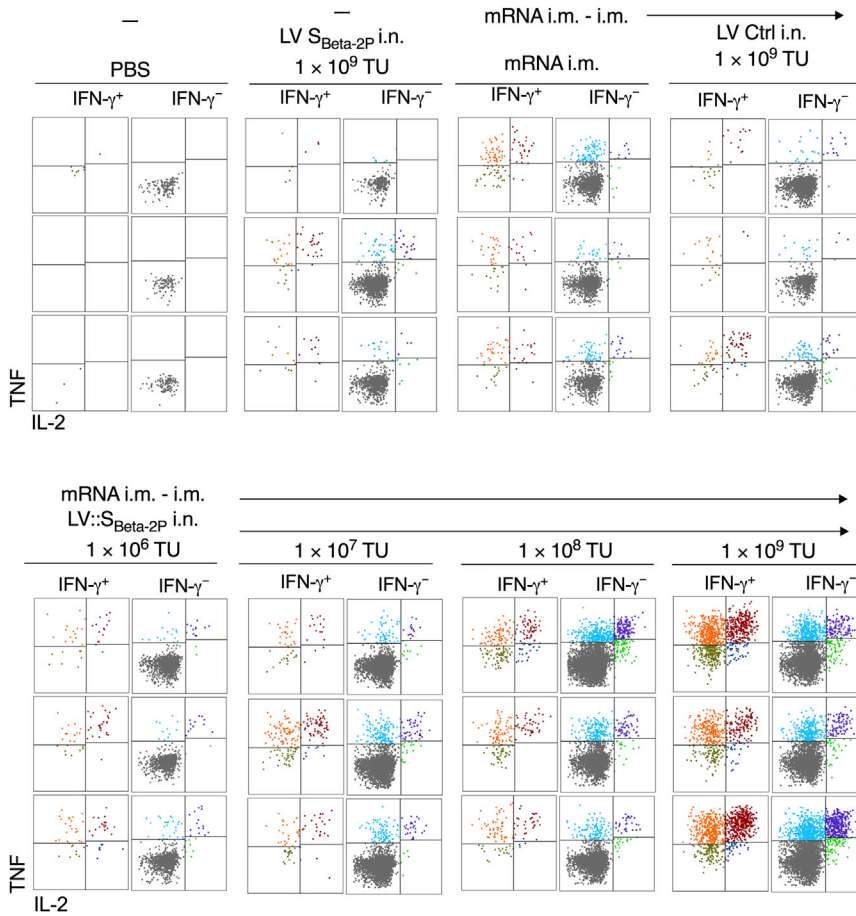


Figure 5. Mucosal CD8⁺ T cell responses to S_{CoV-2} in mRNA-vaccinated mice that were further i.n. boosted with LV::S_{Beta-2P}

The mice are those detailed in Figure 2. (A) Representative IFN- γ response by lung CD8⁺ T cells detected by intracellular cytokine staining after *in vitro* stimulation with a pool of S:256-275, S:536-550, and S:576-590 peptides. Cells are gated on alive CD45⁺ CD8⁺ T cells.

number of somatic hypermutations. Collectively, it seems that there exists some common paratopes in such S_{Beta}-elicited cross-reactive antibodies that interact with the Y501 mutation found in RBD of Alpha, Beta, and Gamma.³⁴

In mice primed and boosted with mRNA vaccine (encoding the ancestral S_{CoV-2} sequence), with waning (cross-) sero-neutralization capabilities, we used escalating doses of LV::S_{Beta-2P} for an i.n. late boost. We demonstrated a dose-dependent increase in anti-S_{CoV-2} IgG and IgA titers, and a broadened sero-neutralization potential both in the sera and lung homogenates against VOCs. No anti-S_{CoV-2} IgA was detected in the lungs of mice injected with the third dose of 1 μ g mRNA given via i.m. injection. Increasing proportions of non-circulating Brm, defined as class-switched surface IgM⁻/IgD⁻ plasma cells, with a CD38⁺ CD73⁺ CD62L⁺ CD69⁺ CD80⁺ phenotype,^{21,22} were detected in a dose-dependent manner, in the lungs of mice boosted i.n. with LV::S_{Beta-2P}.

vaccination has been shown by several teams to be the best at decreasing viral contents in nasal swabs and nasal olfactory neuroepithelium,^{31,32} which can contribute to blocking the respiratory chain of SARS-CoV-2 transmission. One of the advantages of LV-based immunization is the induction of strong T cell immune responses with high cross-reactivity of T cell epitopes from the spikes of diverse VOCs. Therefore, when the neutralizing antibodies fail or wane, the T cell arm of the response remains largely protective, as we recently described in antibody-deficient, B cell-compromised μ MT KO mice.³ This property is relative to a high-quality and long-lasting T cell immunity induced against multiple preserved T cell epitopes, despite the mutations accumulated in the spikes of the emerging VOCs,³ including the Omicron variant.

In the present study, we down-selected the S_{Beta-2P} antigen, which induced the greatest neutralization breadth against the main SARS-CoV-2 VOCs and designed a non-integrative LV encoding a stabilized version of this antigen. The induction of highly cross-reactive neutralizing antibodies by the SARS-CoV-2 Beta variant has been well documented.³³ The notable ability of S_{Beta} to elicit cross-reactive antibodies correlates with (i) the shared genetic and structural features of these antibodies, (ii) their preferential use of specific germline sequences, such as VH1-58 and VH4-39, and (iii) their relatively low

Spike-specific, effector lung CD8⁺ Tc1 cells were largely detected in the initially mRNA-primed and -boosted mice that received a late i.n. LV::S_{Beta-2P} boost. These lung CD8⁺ T cells did not display a Tc2 phenotype. Increasing proportions of lung CD8⁺ CD44⁺ CD69⁺ CD103⁺ Trm were also detected, in a dose-dependent manner, only in LV::S_{Beta-2P} i.n. boosted mice. The systemic CD8⁺ T cell responses against various immunogenic regions of S_{CoV-2} were also increased with 1 \times 10⁸ or 1 \times 10⁹ TU doses of LV::S_{Beta-2P} i.n. boost in the initially mRNA-primed and -boosted mice. The highest i.n. dose of LV::S_{Beta-2P} was comparable with the third injection of 1 μ g/mouse of mRNA given by i.m. injection. The fact that the i.n. administration of LV::S_{Beta-2P} had a substantial boost effect on the systemic T cell immunity indicates that this boost pathway is not at the expense of the induction of systemic immunity. As we recently determined by epitope mapping and cytometric analysis, LV::S immunization only induced CD8⁺—but not CD4⁺—T cells against S_{CoV-2}.² This results from direct transduction of antigen-presenting cells by LVs and thus efficient antigen routing to the major histocompatibility (MHC)-I machinery, but not to the endocytic and MHC-II presentation pathway (our unpublished observation). Furthermore, as LVs are

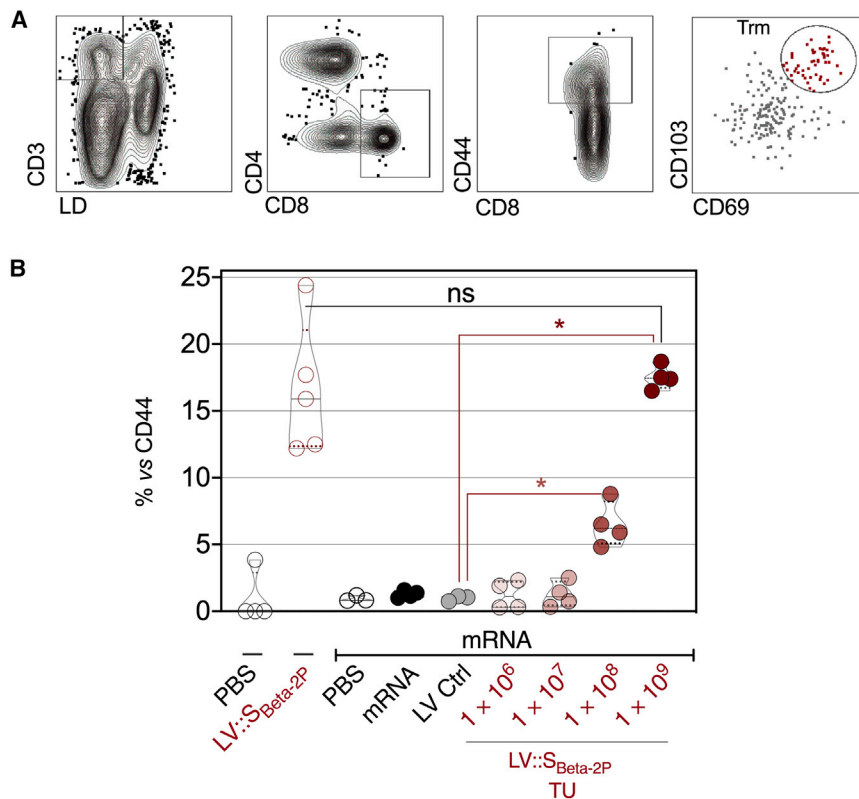


Figure 6. Lung T resident memory subset in mRNA-vaccinated mice that were further i.n. boosted with LV::S_{Beta-2P}

The mice are those detailed in Figure 2. Mucosal immune cells were studied 2 weeks after an LV::S_{Beta-2P} i.n. boost. (A) Cytometric gating strategy to detect lung CD8⁺ T resident memory (CD44⁺CD69⁺CD103⁺), and (B) percentages of this subset among CD8⁺ CD44⁺ T cells in mRNA-vaccinated mice that were further i.n. boosted with LV::S_{Beta-2P}. Statistical significance was evaluated by the Mann-Whitney test (*p < 0.05).

immune memory from remote anatomical sites and the recruitment of the immune arsenal from these sites. In human populations, such a scenario would lead to a high possibility of viral replication and variable levels of its transmission, which would prevent the epidemic from being completely contained by mass vaccination through the systemic route.

It is not yet known if a single third booster will extend and maintain the protective potential, or whether semi-regular boosters will be required against COVID-19 in the future. The LV::S_{Beta-2P} i.n. boost strengthens the intensity, broadens the VOC cross-recognition, and targets B- and T cell immune responses to the principal entry point of SARS-CoV-2, i.e., to the mucosal respiratory tract of the host organism preventing the infection of main anatomical sites. It is interesting to note that in rodents only a pair of cervical ganglia exists *versus* a large network of such ganglia in humans.³⁵ After i.n. immunization, this anatomical feature in humans may provide an even more consistent site of immune response induction and local memory maintenance, at the vicinity of to the potential site of airway infection. In addition, nasopharynx-associated lymphoid tissue is a powerful defense system composed of (i) organized lymphoid tissue, i.e., tonsils, and (ii) diffuse nose-associated lymphoid tissues, where effector and memory B and T lymphocytes are able to maintain long-lasting immunity.³⁶ This mucosal immune arsenal deserves to be explored in the control of SARS-CoV-2 transmission in the current context of the pandemic. A phase I clinical trial is currently in preparation for the use of an i.n. boost by LV::S_{Beta-2P} in previously vaccinated humans or in COVID-19 convalescents. Although LVs cause very little or nearly no inflammation¹⁰ (J.L. and L.M., unpublished observation), to ensure that an i.n. vaccination with LV::S_{Beta-2P} will not result in brain inflammation, we plan to evaluate the toxicity of the preclinical GMP batch in regulatory preclinical assays. We will pay particular attention to the (i) biodistribution of LV::S_{Beta-2P}, to be assessed by PCR and (ii) histopathology in as many organs as possible, including the brain, after i.n. administration of the highest dose planned for the clinical trial and according to kinetics pre-established in non-regulatory preclinical experiments.

not cytopathic, the initially transduced antigen-presenting cells should not generate marked amounts of cell debris that could be taken up by secondary antigen-presenting cells for MHC-II presentation.

Evaluation of the protection in mRNA-primed and -boosted mice showed that, 20 weeks after the first injection of mRNA vaccine, there was no protection detectable in the lungs against infection with the SARS-CoV-2 Delta variant. Importantly, an i.n. boost at week 15 with a dose of 1×10^8 TU/mouse LV::S_{Beta-2P} resulted in full inhibition of SARS-CoV-2 replication in the lungs upon challenge with the Delta variant at week 20. In the mice receiving a 1- μ g mRNA i.m. boost at week 15, the lung SARS-CoV-2 RNA contents was decreased in a statistically comparable manner, albeit without total inhibition of viral replication in all mice.

The lack of protection against the Delta variant infection only 4 months after the initial systemic prime boost by mRNA vaccine, as we observed in the preclinical model in this study, may be explained by the weak efficiency of the ancestral S_{CoV-2} sequence to induce long-lasting neutralizing antibodies against the recent VOCs. In addition, it can be hypothesized that the adaptive immune memory induced by i.m. mRNA immunization is likely to be localized in secondary lymphoid organs at anatomical sites located far from the upper respiratory tract. In such a context, the extraordinary rapid replication of new VOCs, such as Delta or Omicron, in the upper respiratory tract would not leave enough time for the reactivation of im-

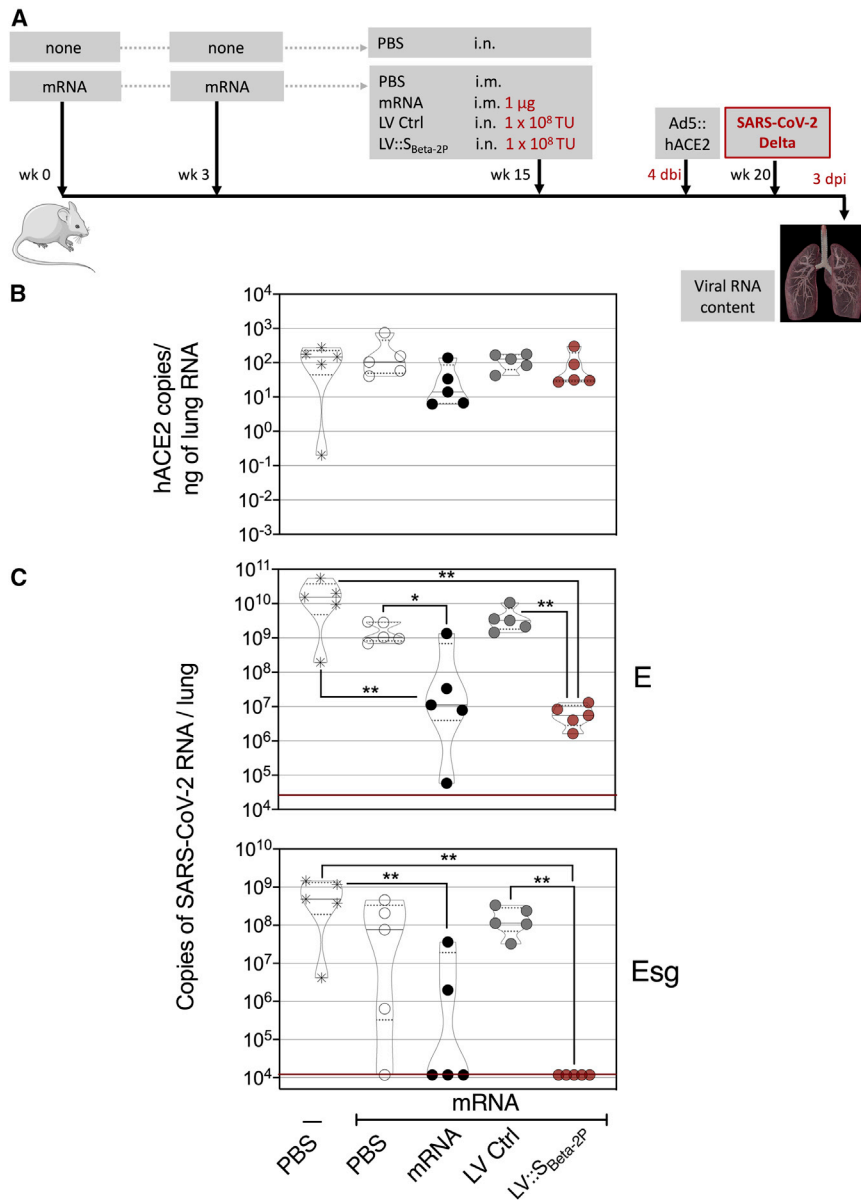


Figure 7. Full protective capacity of LV::S_{Beta-2P} i.n. boost against the Delta variant in initially mRNA-primed and boosted mice

(A) Timeline of mRNA i.m.-i.m. prime-boost vaccination in C57BL/6 mice that were later immunized i.n. with 1×10^8 TU/mouse of LV::S_{Beta-2P} ($n = 4-5$ /group), pre-treated i.n. with Ad5::hACE-2 4 days before i.n. challenge with 0.3×10^5 TCID₅₀ of SARS-CoV-2 Delta variant. (B) Comparative quantification of hACE-2 mRNA in the lungs of Ad5::hACE-2 pre-treated mice at 3 days after infection. (C) Lung viral RNA contents, evaluated by conventional E-specific (top) or sub-genomic Esg-specific (bottom) qRT-PCR at 3 days after infection. Red lines indicate the detection limits. Statistical significance was evaluated by the Mann-Whitney test (* $p < 0.05$, ** $p < 0.01$).

antigens. This may be the reason why LVs are effective at much lower doses compared to adenoviral vectors. The doses of 1×10^8 or 1×10^9 TU are optimal in mice. However, *Mus musculus* species underestimates the efficacy of HIV-based LVs because of restriction factors, which decreases the transduction efficiency of LVs in the murine cells. In larger animals such as piglets,³⁷ horses (P.C., unpublished results), and macaques,³⁸ as well as in humans,⁹ the same range of LV doses are largely effective for the induction of T cell responses and protection *versus* 1×10^{13} adenoviral active particles for human vaccination.⁶

MATERIALS AND METHODS

Mice immunization and SARS-CoV-2 infection

Female C57BL/6J mice were purchased from Janvier, housed in individually ventilated cages under specific pathogen-free conditions at the Institut Pasteur animal facilities, and used at the age of 7 weeks. Mice were immunized i.m. with 1 μ g/mouse mRNA-1273 (Moderna)

vaccine. The Moderna vaccine was provided by the Institut Pasteur Medical Center. These were leftover unusable vaccines in thawed vials that were not authorized to be pooled for human vaccination and would have been destroyed. Thus, the doses used in this study did not deprive any individual of a vaccine dose during the pandemic. For i.n. injections with LV, mice were anesthetized by i.p. injection of ketamine (Imalgene, 80 mg/kg) and xylazine (Rompun, 5 mg/kg). For protection experiments against SARS-CoV-2, mice were transferred into filtered cages in isolator. Four days before SARS-CoV-2 inoculation, mice were pretreated with 3×10^8 IGU of Ad5::hACE2 as previously described.² Mice were then transferred into a level 3 biosafety cabinet and inoculated i.n. with 0.3×10^5 TCID₅₀ of the Delta variant of SARS-CoV-2 clinical isolate³⁹

We have completed a technology transfer to an industrial partner and are now able to produce LVs in large quantities for clinical trials that will be starting soon. After the successful completion of phase I trials, we plan to move to fermenter production, which is now possible for LV production in adherent HEK293-T cells. We have also established the high stability of the LVs if appropriate conservation buffers are used. Compared with adenoviral vectors, LVs have the advantage of being only scarcely inflammatory and not being targets of pre-existing immunity in human populations.^{6,10} LVs have a particular tropism for dendritic cells, which generates endogenous antigen expression in these antigen-presenting cells, whereas adenoviral vectors preferentially target epithelial cells, which requires indirect and cross-presentation of

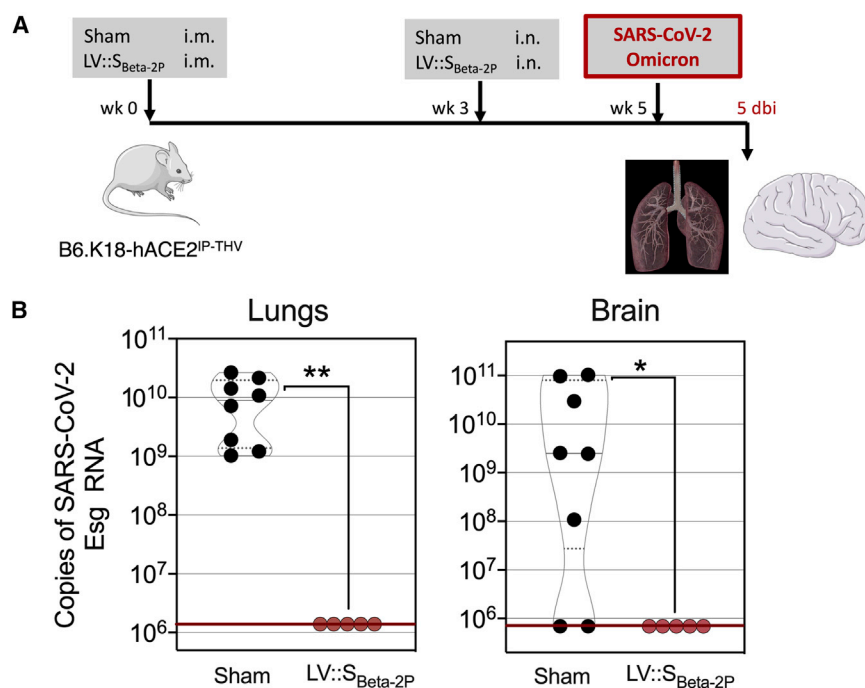


Figure 8. Full protective capacity of LV::SBeta-2P used in a prime (i.m.) boost (i.n.) regimen against the Omicron variant

(A) Timeline of prime-boost vaccination and i.n. challenge with 0.3×10^5 TCID₅₀ of SARS-CoV-2 Omicron variant in B6.K18-hACE2^{IP-THV} transgenic mice ($n = 5/\text{group}$). (B) Lung viral RNA contents, evaluated by sub-genomic Esg-specific qRT-PCR at 5 days after infection. Red lines indicate the detection limits. Statistical significance was evaluated by the Mann-Whitney test (* $p < 0.05$, ** $p < 0.01$).

contained in 20 μL . B6.K18-hACE2^{IP-THV} mice³ were primed i.m. and boosted i.n. by LV::SBeta-2P and then inoculated with 0.3×10^5 TCID₅₀ of the Omicron BA.1 variant of SARS-CoV-2 clinical isolate.²⁷ Mice were then housed in filtered cages in an isolator in BioSafety Level 3 animal facilities. The organs recovered from the infected animals were manipulated according to the approved standard procedures of these facilities.

Ethical approval of animal experimentation

Experimentation on animals was performed in accordance with the European and French guidelines (Directive 86/609/CEE and Decree 87-848 of 19 October 1987) subsequent to approval by the Institut Pasteur Safety, Animal Care and Use Committee, protocol agreement delivered by local ethical committee (CETEA #DAP20007, CETEA #DAP200058) and Ministry of High Education and Research APAFIS#24627-2020031117362508 v1, APAFIS#28755-2020122110238379 v1.

Construction and production of vaccinal LV::SBeta-2P

First, a codon-optimized sequence of spike from the ancestral, D614G, Alpha, Beta, or Gamma VOCs were synthesized and inserted into the pMK-RQ_S-2019-nCoV_S501YV2 plasmid. The S sequence was then extracted by BamHI/XhoI digestion to be ligated into the pFlap lentiviral plasmid between the BamHI and XhoI restriction sites, located between the native human ieCMV promoter and the mutated *atg* starting codon of the Woodchuck post-transcriptional regulatory element (WPRE) sequence (Figure S5). To introduce the K⁹⁸⁶P-V⁹⁸⁷P “2P” double mutation in S_{D614G} or S_{Beta}, a directed mutagenesis was performed by use of Takara In-Fusion kit on the corresponding pFlap plasmids.

Various pFlap-ieCMV-S-WPREm or pFlap-ieCMV-S_{2P}-WPREm plasmids were amplified and used to produce non-integrative vaccinal LV, as previously described.^{2,6} The envelope plasmid encodes VSV-G under ieCMV promoter and the packaging plasmid contains *gag*, *pol*, *tat*, and *rev* genes. The integrase resulting from this plasmid carries a missense amino acid in its catalytic triad, i.e., the D64V mutation, that prevents the integration of viral DNA into the host chromosome.

Without integration, the viral DNA remains in an episomal form, very effective for gene expression.^{2,6}

Analysis of humoral and systemic T cell immunity

Anti-S_{CoV-2} IgG and IgA antibody titers were determined by ELISA by use of recombinant stabilized S_{CoV-2} or RBD fragment for coating. The neutralization potential of clarified and decomplexed sera or lung homogenates was quantitated by use of lentiviral particles pseudo-typed with S_{CoV-2} from diverse variants, as previously described.^{2,40}

T-splenocyte responses were quantitated by IFN- γ ELISPOT after *in vitro* stimulation with S:256-275, S:536-550, or S:576-590 synthetic 15-mer peptides, which contain S_{CoV-2} MHC-I-restricted epitopes in H-2^d mice.² Spots were quantified in a CTL Immunospot S6 ultimate-V Analyser by use of CTL Immunocapture 7.0.8.1 program.

Phenotypic and functional cytometric analysis of lung immune cells

The enrichment and staining of lung immune cells were performed as detailed previously^{2,3} after treatment with 400 U/mL type IV collagenase and DNase I (Roche) for a 30-min incubation at 37°C and homogenization by use of GentleMacs (Miltenyi Biotech). Cell suspensions were then filtered through 100 μm -pore filters, centrifuged at 1,200 rpm and enriched on Ficoll gradient after 20 min centrifugation at 3,000 rpm at room temperature, without breaks. The recovered cells were co-cultured with syngeneic bone marrow-derived dendritic cells loaded with a pool of A, B, and C peptides, each at 1 $\mu\text{g}/\text{mL}$ or negative control peptide at 3 $\mu\text{g}/\text{mL}$. The following mixture was used to detect lung Tc1 cells: PerCP-Cy5.5-anti-CD3 (45-0031-82,

eBioScience), eF450-anti-CD4 (48-0042-82, eBioScience), and APC-anti-CD8 (17-0081-82, eBioScience) for surface staining and BV650-anti-IFN- γ (563854, BD), FITC-anti-TNF (554418, BD), and PE-anti-IL-2 (561061, BD) for intracellular staining. The following mixture was used to detect lung Tc2 cells: PerCP-Cy5.5-anti-CD3 (45-0031-82, eBioScience), eF450-anti-CD4 (48-0042-82, eBioScience), and BV711-anti-CD8 (563046, BD Biosciences) for surface staining and BV605-anti-IL-4 (504125, BioLegend Europe BV), APC-anti-IL-5 (504306, BioLegend Europe BV), FITC-anti-IL-10 (505006, BioLegend Europe BV), and PE-anti-IL-13 (12-7133-81, eBioScience) for intracellular staining. The intracellular staining was performed by use of the Fix Perm kit (BD Biosciences), following the manufacturer's protocol. Dead cells were excluded by use of Near IR Live/Dead (Invitrogen). Staining was performed in the presence of Fc γ II/III receptor blocking anti-CD16/CD32 (BD Biosciences).

To identify lung-resident memory CD8⁺ T cell subsets, a mixture of PerCP-Vio700-anti-CD3 (130-119-656, Miltenyi Biotec), PECy7-CD4 (552775, BD Biosciences), BV510-anti-CD8 (100752, BioLegend), PE-anti-CD62L (553151, BD Biosciences), APC-anti-CD69 (560689, BD Biosciences), APC-Cy7-anti-CD44 (560568, BD Biosciences), FITC-anti-CD103 (11-1031-82, eBiosciences), and yellow Live/Dead (Invitrogen) was used. Lung Brm were studied by surface staining with a mixture of PerCP Vio700-anti-IgM (130-106-012, Miltenyi), and PerCP Vio700-anti-IgD (130-103-797, Miltenyi), APC-H7-anti-CD19 (560143, BD Biosciences), PE-anti-CD38 (102708, BioLegend Europe BV), PE-Cy7-anti-CD62L (ab25569, AbCam), BV711-anti-CD69 (740664, BD Biosciences), BV421-anti-CD73 (127217, BioLegend Europe BV), and FITC-anti-CD80 (104705, BioLegend Europe BV and yellow Live/Dead (Invitrogen).

Cells were incubated with appropriate mixtures for 25 min at 4°C, washed in PBS containing 3% fetal calf serum and fixed with paraformaldehyde 4% after an overnight incubation at 4°C. Samples were acquired in an Attune NxT cytometer (Invitrogen) and data analyzed by FlowJo software (Treestar).

Determination of viral RNA content in the organs

Organs from mice were removed and immediately frozen at -80°C on dry ice. RNA from circulating SARS-CoV-2 was prepared from lungs as described previously.² Lung homogenates were prepared by thawing and homogenizing in lysing matrix M (MP Biomedical) with 500 μL of PBS using an MP Biomedical Fastprep 24 Tissue Homogenizer. RNA was extracted from the supernatants of organ homogenates centrifuged during 10 min at 2,000g using the Qiagen Rneasy kit. The RNA samples were then used to determine viral RNA content by E-specific qRT-PCR. To determine viral RNA content by Esg-specific qRT-PCR, total RNA was prepared using lysing matrix D (MP Biomedical) containing 1 mL TRIzol reagent (ThermoFisher Scientific) and homogenization for 30 s at 6.0 m/s twice using MP Biomedical Fastprep 24 Tissue Homogenizer. The quality of RNA samples was assessed by use of a Bioanalyzer 2100 (Agilent Technologies). Viral RNA contents were quantitated using a NanoDrop Spectrophotometer (ThermoFisher Scientific NanoDrop). The RNA Integrity Number was 7.5–10.0. SARS-

CoV-2 E or E sub-genomic mRNA were quantitated after reverse transcription and real-time quantitative TaqMan PCR, using SuperScript III Platinum One-Step qRT-PCR System (Invitrogen) and specific primers and probe (Eurofins), as recently described.³

Lung histology

Left lobes from lungs were fixed in formalin and embedded in paraffin. Paraffin sections (5- μm thick) were stained with H&E. Slides were scanned using the AxioScan Z1 (Carl Zeiss Meditec) system and images were analyzed with the Zen 2.6 software. Histological images were evaluated according to a score of 0–5 (normal, minimal, mild, moderate, marked, or severe).

Statistical methods

Statistical significance of the differences was determined by Mann-Whitney test by use of Prism GraphPad.

SUPPLEMENTAL INFORMATION

Supplemental information can be found online at <https://doi.org/10.1016/j.ymthe.2022.04.016>.

ACKNOWLEDGMENTS

The authors are grateful to Dr. Marie José Quentin-Millet and Estelle Besson (TheraVectys) for discussion and advice, to Magali Tichit and Sabine Maurin for excellent technical assistance in preparing histological sections, to Sébastien Chardenoux (CIGM, Institut Pasteur) for excellent technical assistance in B6.K18-hACE2^{IP-THV} mouse transgenesis, and to Marie Laure Loriquet and Dr. Paul-Henri Consigny (Institut Pasteur Medical Center) for their gift of the leftover Moderna vaccines, not unusable in humans, so that this study did not deprive any individual of a vaccine dose during the COVID-19 pandemic. The SARS-CoV2 variant Delta/2021/I7.2 200 was supplied by the Virus and Immunity Unit (Institut Pasteur, Paris, France) headed by Olivier Schwartz. The SARS-CoV-2 Omicron BA.1 variant was initially supplied by the Virus and Immunity Unit (Institut Pasteur, Paris, France) headed by Olivier Schwartz, and was provided to our laboratory by Matthieu Prot and Etienne Simon-Lorière (G5 Evolutionary Genomics of RNA Viruses, Institut Pasteur, Paris, France). This work was supported by TheraVectys and the Institut Pasteur.

AUTHOR CONTRIBUTIONS

B.V., J.L., C.G., M.B., L.M., and P.C. conceptualized and designed the study; B.V., J.L., A.N., P.A., I.F., F.L.C., F.M., K.N., M.B., and L.M. acquired data; A.N., F.M., C.B., and F.A. designed, constructed, and produced lentiviral or adenoviral vectors; F.G. and D.H. performed histology; C.P. and H.M. provided recombinant Spike protein; F.L.V. collaboratively generated B6.K18-hACE2^{IP-THV} transgenic mice; B.V., J.L., F.A., M.B., L.M., and P.C. analyzed and interpreted the data; and L.M. wrote the paper.

DECLARATION OF INTERESTS

P.C. is the founder and CSO of TheraVectys. B.V., A.N., P.A., I.F., F.L.C., F.M., K.N., and F.A. are employees of TheraVectys. L.M. has a consultancy activity for TheraVectys. The other authors declare

no competing interests. P.A., I.F., J.L., B.V., F.A., M.B., L.M., and P.C. are the inventors of pending patents directed to the potential of i.n. LV::S vaccination against SARS-CoV-2.

REFERENCES

- https://cdn.who.int/media/docs/default-source/immunization/sage/covid/global-covid-19-vaccination-strategic-vision-for-2022_sage-yellow-book.pdf?sfvrsn=4827ec0d_5.
- Ku, M.W., Bourguin, M., Authie, P., Lopez, J., Nemirov, K., Moncoq, F., Noirat, A., Vesin, B., Nevo, F., Blanc, C., et al. (2021). Intranasal vaccination with a lentiviral vector protects against SARS-CoV-2 in preclinical animal models. *Cell Host Microbe* 29, 236–249.e6. <https://doi.org/10.1016/j.chom.2020.12.010>.
- Ku, M.W., Authie, P., Bourguin, M., Anna, F., Noirat, A., Moncoq, F., Vesin, B., Nevo, F., Lopez, J., Souque, P., et al. (2021). Brain cross-protection against SARS-CoV-2 variants by a lentiviral vaccine in new transgenic mice. *EMBO Mol. Med.* 13, e14459. <https://doi.org/10.15252/emmm.202114459>.
- Juno, J.A., and Wheatley, A.K. (2021). Boosting immunity to COVID-19 vaccines. *Nat. Med.* 27, 1874–1875. <https://doi.org/10.1038/s41591-021-01560-x>.
- Hu, B., Tai, A., and Wang, P. (2011). Immunization delivered by lentiviral vectors for cancer and infectious diseases. *Immunol. Rev.* 239, 45–61. <https://doi.org/10.1111/j.1600-065X.2010.00967.x>.
- Ku, M.W., Charneau, P., and Majlessi, L. (2021). Use of lentiviral vectors in vaccination. *Expert Rev. Vaccin.* 20, 1571–1586. <https://doi.org/10.1080/14760584.2021.1988854>.
- Guermonprez, P., Gerber-Ferder, Y., Vaivode, K., Bourdely, P., and Helft, J. (2019). Origin and development of classical dendritic cells. *Int. Rev. Cell Mol. Biol.* 349, 1–54. <https://doi.org/10.1016/bs.ircmb.2019.08.002>.
- Ku, M.W., Authie, P., Nevo, F., Souque, P., Bourguin, M., Romano, M., Charneau, P., and Majlessi, L. (2021). Lentiviral vector induces high-quality memory T cells via dendritic cells transduction. *Commun. Biol.* 4, 713. <https://doi.org/10.1038/s42003-021-02251-6>.
- TheraVectys-Clinical-Trial. (2019). Safety, Tolerability and Immunogenicity Induced by the THV01 Treatment in Patients Infected with HIV-1 Clade B and Treated with Highly Active Antiretroviral Therapy (HAART). <https://www.clinicaltrialsregister.eu/ctr-search/search?query=2011-006260-52>.
- Cousin, C., Oberkamp, M., Felix, T., Rosenbaum, P., Weil, R., Fabrega, S., Morante, V., Negri, D., Cara, A., Dadaglio, G., and Leclerc, C. (2019). Persistence of integrase-deficient lentiviral vectors correlates with the induction of STING-independent CD8(+) T cell responses. *Cell Rep.* 26, 1242–1257.e7. <https://doi.org/10.1016/j.celrep.2019.01.025>.
- Lund, F.E., and Randall, T.D. (2021). Scent of a vaccine. *Science* 373, 397–399. <https://doi.org/10.1126/science.abg9857>.
- van Doremalen, N., Purushotham, J.N., Schulz, J.E., Holbrook, M.G., Bushmaker, T., Carmody, A., Port, J.R., Yinda, C.K., Okumura, A., Saturday, G., et al. (2021). Intranasal ChAdOx1 nCoV-19/AZD1222 vaccination reduces viral shedding after SARS-CoV-2 D614G challenge in preclinical models. *Sci. Transl. Med.* 13, eabh0755. <https://doi.org/10.1126/scitranslmed.abh0755>.
- Castells, M.C., and Phillips, E.J. (2021). Maintaining safety with SARS-CoV-2 vaccines. *N. Engl. J. Med.* 384, 643–649. <https://doi.org/10.1056/NEJMra2035343>.
- He, Q., Mao, Q., An, C., Zhang, J., Gao, F., Bian, L., Li, C., Liang, Z., Xu, M., and Wang, J. (2021). Heterologous prime-boost: breaking the protective immune response bottleneck of COVID-19 vaccine candidates. *Emerg. Microbes Infect.* 10, 629–637. <https://doi.org/10.1080/22221751.2021.1902245>.
- Lu, S. (2009). Heterologous prime-boost vaccination. *Curr. Opin. Immunol.* 21, 346–351. <https://doi.org/10.1016/j.coi.2009.05.016>.
- Nordstrom, P., Ballin, M., and Nordstrom, A. (2021). Effectiveness of heterologous ChAdOx1 nCoV-19 and mRNA prime-boost vaccination against symptomatic Covid-19 infection in Sweden: a nationwide cohort study. *Lancet Reg. Health Eur.* 11, 100249. <https://doi.org/10.1016/j.lanpep.2021.100249>.
- Jackson, L.A., Anderson, E.J., Roupel, N.G., Roberts, P.C., Makhene, M., Coler, R.N., McCullough, M.P., Chappell, J.D., Denison, M.R., Stevens, L.J., et al. (2020). An mRNA vaccine against SARS-CoV-2 - preliminary report. *N. Engl. J. Med.* 383, 1920–1931. <https://doi.org/10.1056/NEJMoa2022483>.
- Wang, F., Kream, R.M., and Stefano, G.B. (2020). An evidence based perspective on mRNA-SARS-CoV-2 vaccine development. *Med. Sci. Monit.* 26, e924700. <https://doi.org/10.12659/MSM.924700>.
- Walls, A.C., Park, Y.J., Tortorici, M.A., Wall, A., McGuire, A.T., and Veesler, D. (2020). Structure, function, and antigenicity of the SARS-CoV-2 spike glycoprotein. *Cell* 181, 281–292.e6. <https://doi.org/10.1016/j.cell.2020.02.058>.
- Corbett, K.S., Edwards, D.K., Leist, S.R., Abiona, O.M., Boyoglu-Barnum, S., Gillespie, R.A., Himansu, S., Schafer, A., Ziwawo, C.T., DiPiazza, A.T., et al. (2020). SARS-CoV-2 mRNA vaccine design enabled by prototype pathogen preparedness. *Nature* 586, 567–571. <https://doi.org/10.1038/s41586-020-2622-0>.
- Barker, K.A., Etesami, N.S., Shenoy, A.T., Arafa, E.I., Lyon de Ana, C., Smith, N.M., Martin, I.M., Goltry, W.N., Barron, A.M., Browning, J.L., et al. (2021). Lung-resident memory B cells protect against bacterial pneumonia. *J. Clin. Invest.* 131, e141810. <https://doi.org/10.1172/JCI141810>.
- Onodera, T., Takahashi, Y., Yokoi, Y., Ato, M., Kodama, Y., Hachimura, S., Kurosaki, T., and Kobayashi, K. (2012). Memory B cells in the lung participate in protective humoral immune responses to pulmonary influenza virus reinfection. *Proc. Natl. Acad. Sci. U S A* 109, 2485–2490. <https://doi.org/10.1073/pnas.1115369109>.
- Masopust, D., and Soerens, A.G. (2019). Tissue-resident T cells and other resident leukocytes. *Annu. Rev. Immunol.* 37, 521–546. <https://doi.org/10.1146/annurev-immunol-042617-053214>.
- Chandrashekar, A., Liu, J., Martinot, A.J., McMahan, K., Mercado, N.B., Peter, L., Tostanoski, L.H., Yu, J., Maliga, Z., Nekorchuk, M., et al. (2020). SARS-CoV-2 infection protects against rechallenge in rhesus macaques. *Science* 369, 812–817. <https://doi.org/10.1126/science.abc4776>.
- Tostanoski, L.H., Wegmann, F., Martinot, A.J., Loos, C., McMahan, K., Mercado, N.B., Yu, J., Chan, C.N., Bondoc, S., Starke, C.E., et al. (2020). Ad26 vaccine protects against SARS-CoV-2 severe clinical disease in hamsters. *Nat. Med.* 26, 1694–1700. <https://doi.org/10.1038/s41591-020-1070-6>.
- Wolfel, R., Corman, V.M., Guggemos, W., Seilmaier, M., Zange, S., Muller, M.A., Niemeyer, D., Jones, T.C., Vollmar, P., Rothe, C., et al. (2020). Virological assessment of hospitalized patients with COVID-2019. *Nature* 581, 465–469. <https://doi.org/10.1038/s41586-020-2196-x>.
- Planas, D., Saunders, N., Maes, P., Guivel-Benhassine, F., Planchais, C., Buchrieser, J., Bolland, W.H., Porrot, F., Staropoli, I., Lemoine, F., et al. (2022). Considerable escape of SARS-CoV-2 Omicron to antibody neutralization. *Nature* 602, 671–675. <https://doi.org/10.1038/s41586-021-04389-z>.
- Barros-Martins, J., Hammerschmidt, S.I., Cossmann, A., Odak, I., Stankov, M.V., Morillas Ramos, G., Dopfer-Jablonka, A., Heidemann, A., Ritter, C., Friedrichsen, M., et al. (2021). Immune responses against SARS-CoV-2 variants after heterologous and homologous ChAdOx1 nCoV-19/BNT162b2 vaccination. *Nat. Med.* 27, 1525–1529. <https://doi.org/10.1038/s41591-021-01449-9>.
- Kardani, K., Bolhassani, A., and Shahbazi, S. (2016). Prime-boost vaccine strategy against viral infections: mechanisms and benefits. *Vaccine* 34, 413–423. <https://doi.org/10.1016/j.vaccine.2015.11.062>.
- Sette, A., and Crotty, S. (2021). Adaptive immunity to SARS-CoV-2 and COVID-19. *Cell* 184, 861–880. <https://doi.org/10.1016/j.cell.2021.01.007>.
- Bricker, T.L., Darling, T.L., Hassan, A.O., Harastani, H.H., Soung, A., Jiang, X., Dai, Y.N., Zhao, H., Adams, L.J., Holtzman, M.J., et al. (2021). A single intranasal or intramuscular immunization with chimpanzee adenovirus-vectored SARS-CoV-2 vaccine protects against pneumonia in hamsters. *Cell Rep.* 36, 109400. <https://doi.org/10.1016/j.celrep.2021.109400>.
- Hassan, A.O., Feldmann, F., Zhao, H., Curiel, D.T., Okumura, A., Tang-Huau, T.L., Case, J.B., Meade-White, K., Callison, J., Chen, R.E., et al. (2021). A single intranasal dose of chimpanzee adenovirus-vectored vaccine protects against SARS-CoV-2 infection in rhesus macaques. *Cell Rep. Med.* 2, 100230. <https://doi.org/10.1016/j.xcrm.2021.100230>.
- Moyo-Gwete, T., Madzivhandila, M., Makhado, Z., Ayres, F., Mhlanga, D., Oosthuysen, B., Lambson, B.E., Kgagudi, P., Tegally, H., Iranzadeh, A., et al.

- (2021). Cross-reactive neutralizing antibody responses elicited by SARS-CoV-2 501Y.V2 (B.1.351). *N. Engl. J. Med.* 384, 2161–2163. <https://doi.org/10.1056/NEJMc2104192>.
34. Reincke, S.M., Yuan, M., Kornau, H.C., Corman, V.M., van Hoof, S., Sanchez-Sendin, E., Ramberger, M., Yu, W., Hua, Y., Tien, H., et al. (2022). SARS-CoV-2 Beta variant infection elicits potent lineage-specific and cross-reactive antibodies. *Science* 375, 782–787. <https://doi.org/10.1126/science.abm5835>.
35. <https://teachmeanatomy.info/neck/vessels/lymphatics/>.
36. Porzia, A., Cavaliere, C., Begvarfaj, E., Masieri, S., and Mainiero, F. (2018). Human nasal immune system: a special site for immune response establishment. *J. Biol. Regul. Homeost. Agents* 32, 3–8.
37. de Wispelaere, M., Ricklin, M., Souque, P., Frenkiel, M.P., Paulous, S., Garcia-Nicolas, O., Summerfield, A., Charneau, P., and Despres, P. (2015). A lentiviral vector expressing Japanese encephalitis virus-like particles elicits broad neutralizing antibody response in pigs. *PLoS Negl. Trop. Dis.* 9, e0004081. <https://doi.org/10.1371/journal.pntd.0004081>.
38. Beignon, A.S., Mollier, K., Liard, C., Coutant, F., Munier, S., Riviere, J., Souque, P., and Charneau, P. (2009). Lentiviral vector-based prime/boost vaccination against AIDS: pilot study shows protection against Simian immunodeficiency virus SIVmac251 challenge in macaques. *J. Virol.* 83, 10963–10974. <https://doi.org/10.1128/JVI.01284-09>.
39. Planas, D., Veyer, D., Baidaliuk, A., Staropoli, I., Guivel-Benhassine, F., Rajah, M.M., Planchais, C., Porrot, F., Robillard, N., Puech, J., et al. (2021). Reduced sensitivity of SARS-CoV-2 variant Delta to antibody neutralization. *Nature* 596, 276–280. <https://doi.org/10.1038/s41586-021-03777-9>.
40. Sterlin, D., Mathian, A., Miyara, M., Mohr, A., Anna, F., Claer, L., Quentric, P., Fadlallah, J., Devilliers, H., Ghillani, P., et al. (2021). IgA dominates the early neutralizing antibody response to SARS-CoV-2. *Sci. Transl. Med.* 13, eabd2223. <https://doi.org/10.1126/scitranslmed.abd2223>.